Quantum Transducer Using a Parametric Driven-Dissipative Phase Transition

Toni L. Heugel, Matteo Biondi, Oded Zilberberg, and R. Chitra
Institute for Theoretical Physics, ETH Zurich, 8093 Zürich, Switzerland

(Received 22 December 2018; published 23 October 2019)

We study a dissipative Kerr resonator subject to both single- and two-photon detuned drives. Beyond a critical detuning threshold, the Kerr resonator exhibits a semiclassical first-order dissipative phase transition between two different steady states that are characterized by a π phase switch of the cavity field. This transition is shown to persist deep into the quantum limit of low photon numbers. Remarkably, the detuning frequency at which this transition occurs depends almost linearly on the amplitude of the single-photon drive. Based on this phase-switching feature, we devise a sensitive quantum transducer that translates the observed frequency of the parametric quantum phase transition to the detected single-photon amplitude signal. The effects of noise and temperature on the corresponding sensing protocol are addressed, and a realistic circuit-QED implementation is discussed.

DOI: 10.1103/PhysRevLett.123.173601

Introduction.—Phase transitions are commonly associated with strongly enhanced susceptibilities. Proximity to phase transitions, therefore, renders systems highly sensitive to external perturbations. Harnessing this augmented sensitivity for sensing and metrology using quantum systems [1] has been the focus of numerous recent efforts in diverse settings, e.g., equilibrium systems [2], PT-symmetric cavities [3], dynamical phase transitions [4], and lasers [5]. From this perspective, quantum driven-dissipative systems offer a fertile platform to devise such rich sensing protocols. These systems are at the avantgarde of contemporary research at the interface between condensed matter physics and quantum optics [6,7]. The dynamics of these intrinsically nonequilibrium systems is richer than that of their equilibrium counterparts, and dissipative phase transitions (DPTs) between different out-of-equilibrium phases can be controllably tuned. DPTs can be realized in various platforms, including cold atoms [8], trapped ions [9], superconducting circuits [10], and exciton-polariton cavities [11].

A paradigmatic example of a nonequilibrium phase transition occurs in driven-dissipative nonlinear Kerr oscillators: In the semiclassical limit of large photon numbers and as a function of single-photon drive detuning, this system undergoes a first-order transition manifesting as a bistability in photon numbers [12–16]. Applying instead a two-photon drive, the resulting Kerr parametric oscillator (KPO) with weak single-photon losses exhibits an additional continuous transition related to the appearance of a parametron which can exist in either of two coherent states of equal amplitude but π-phase shifted with respect to each other [17–19]. At low photon numbers, these coherent states can be recomposed into Schrödinger cat states of opposite parities and have been proposed as a new resource for universal quantum computation [20–22]. Concurrently, optimization algorithms based on annealing with parametrons have recently been demonstrated using a classical KPO network [23] with promising quantum extensions [24].

In this Letter, we propose a quantum sensing scheme based on a first-order symmetry-breaking DPT. This DPT stems from an explicit breaking of the parity symmetry by the single-photon drive, resulting in an abrupt switching between the coherent states. It is also characterized by a vanishing Liouvillian spectral gap [25]. This transition is the quantum manifestation of the classical parametric symmetry breaking studied in Refs. [26–28]. Here, we find that at low and intermediate photon numbers this switching persists as a sharp crossover. Our measurement protocol extracts the *unknown* amplitude of an external coherent (or single-photon) drive (signal) from the detuning frequency at which the KPO switches from one coherent state to the other. Remarkably, the switching frequency scales linearly with the amplitude of the single-photon drive, thus realizing a quantum transducer. Such a coherent tone depends on the actual physical realization of the KPO and can emerge from a plethora of processes such as microwave sources [10], external lasers [6], weak electrical fields, optical dipole forces, spin-dependent forces [29], etc. Furthermore, we discuss the impact of quantum noise on the transducer's sensitivity by simulating a heterodyne detection protocol and by analyzing finite-temperature effects. Our results reiterate in a quantum setting the robustness and potential of our detection scheme. Lastly, our scheme is operational in a wide range of parameters and readily realizable in contemporary quantum engineered settings, e.g., in circuit QED, where parametric driving is already utilized for Josephson parametric amplifiers [30].

Model.—The quantum KPO [Fig. 1(a)] is described by the Hamiltonian ($\hbar = 1$)

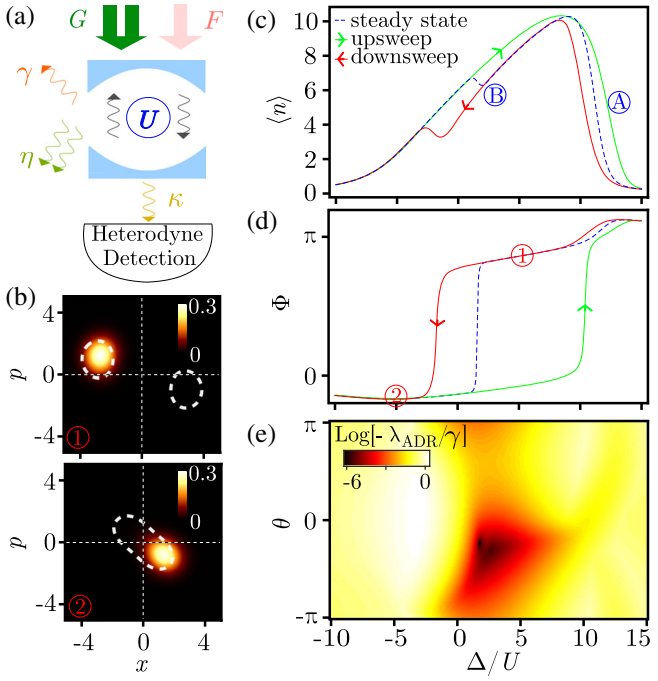

FIG. 1. (a) Schematic representation of a KPO with nonlinearity U and loss rates γ and η subject to single- and two-photon drives F and G, respectively. The emitted photons by the cavity with rate κ are collected by a heterodyne detector. (b) Steady-state Husimi Q functions at points ① and ②; cf. (c) and (d). Dashed lines mark the contour of the $F = 0$ Q function. (c),(d) Photon density $\langle n\rangle$ and phase Φ of the cavity field, as a function of detuning Δ/U in the steady state (dashed blue line) and for upsweeps (green) and downsweeps (red) of Δ/U, obtained from Eq. (2). At large positive Δ/U, the KPO crosses over from high $\langle n\rangle$ to low $\langle n\rangle$. At $\Delta \approx 0$ [marked by Ⓑ] in (c), we see a kink in the steady state $\langle n\rangle$ concomitant with a π switch in the phase (d). The kink and phase switch are also seen for downsweeps. (e) The Liouvillian gap as a function of Δ/U and phase θ of G. The gap vanishes at the phase-switching transition, marking the onset of a quantum DPT. System parameters are $F/U = 4$, $|G|/U = 6$, $\gamma/U = 0.5$, and $\eta/U = 0.5$. $\theta = -(\pi/2)$ in (c) and (d). Δ/U is swept linearly from $\Delta_1/U = -10$ to $\Delta_2/U = 15$ and vice versa in a total sweep time $t_s = 50/U$.

$$H = -\Delta n + \frac{U}{2}n(n-1) - \left(Fa + \frac{G^*}{2}a^2 + \text{H.c.}\right) \quad (1)$$

in terms of the bosonic operator a and the number operator $n = a^\dagger a$. The KPO is parametrically pumped with strength G, while F is the strength of the single-photon drive; without the loss of generality, we set F to be real and $G = |G|\exp(i\theta)$. Equation (1) is written in a frame rotating with respect to the single-photon drive frequency ω_d, and, thus, the bare cavity frequency ω_c is renormalized to the detuning $\Delta = \omega_d - \omega_c$. The parametric modulation is fixed at $2\omega_d$, and U is the Kerr nonlinearity. The dissipative dynamics for the density matrix ρ is determined by the Lindblad master equation

$$\dot{\rho} = \mathcal{L}\rho \equiv -i[H,\rho] + \gamma\mathcal{D}[a]\rho + \eta\mathcal{D}[a^2]\rho, \quad (2)$$

where $\mathcal{L}$ is the Liouvillian superoperator, γ and η are, respectively, the single- and two-photon decay rates, and $\mathcal{D}[O]\rho = O\rho O^\dagger - \frac{1}{2}O^\dagger O\rho - \frac{1}{2}\rho O^\dagger O$.

Steady state and dynamics.—When the system is subject solely to a two-photon drive, $F = 0, G \neq 0$, the system has a $\mathcal{Z}_2$ symmetry associated with the parity operator $e^{i\pi a^\dagger a}$. For a wide range of typical experimental parameters, the steady state is given by $\rho_{\text{steady}} = c_+|C_+\rangle\langle C_+| + c_-|C_-\rangle\langle C_-|$, where the cat states $|C_\pm\rangle = c_N(|\alpha\rangle \pm |-\alpha\rangle)$, with weighting $c_\pm$, are represented by the coherent states $|\pm\alpha\rangle$ with normalization c_N [17,18]. Defining the Husimi quasiprobability distribution function $Q(x,p) = (1/\pi)\langle x+ip|\rho|x+ip\rangle$, where $|x+ip\rangle \equiv |\alpha\rangle$, the $\mathcal{Z}_2$ symmetry manifests in the steady state as $Q(x,p) = Q(-x,-p)$ [dashed lines in Fig. 1(b)]. For $G \gtrsim \gamma, \eta$ and a wide range of detuning around $\Delta \approx 0$, the Q function is bimodal, indicating the formation of cat states. For a large enough $|G|$, the system is known to exhibit both a first-order DPT reflecting classical bistability and a continuous DPT related to the appearance of bimodality in the Q function [19,31].

We now investigate the interplay between the one- and two-photon drives as their detunings are jointly varied. Since the single-photon drive breaks the $\mathcal{Z}_2$ symmetry, the coherent states $|\pm\alpha\rangle$ contribute unequally to ρ [19]. In Fig. 1(c), we plot the photon number $\langle n\rangle$ as a function of Δ/U. The steady-state photon number is low at large detunings $|\Delta/U| \gg 1$ and increases to a maximum at $\Delta/U \approx 10$, followed by a pronounced drop [see Ⓐ in Fig. 1(c)]. Interestingly, we observe a kink occurring at $\Delta/U \approx 0$ [see Ⓑ]. This kink is a precursor to the continuous DPT discussed earlier, which is now discontinuous due to the symmetry-breaking F.

This feature is strongly reflected in the phase of the cavity field $\Phi = \arctan[p/x]$, where $x = \langle a + a^\dagger\rangle$ and $p = \langle -i(a - a^\dagger)\rangle$. In Fig. 1(d), we see that the phase abruptly switches by π in the vicinity of $\Delta/U \approx 0$. This phase switch stems directly from the transition between the two modes of the parametron in the Q function. Note that these modes are now shifted by the single-photon drive but nonetheless remain in opposing quadrants of the Q function [Fig. 1(b)]. The origin of this effect can be traced back to the bifurcation physics in the classical limit of the model [26–28].

To substantiate the link between the phase jump and DPTs, it is instructive to look at the Liouvillian gap λ_{ADR} in the Liouvillian spectrum [Fig. 1(e)]. All eigenvalues λ of the Liouvillian superoperator $\mathcal{L}$ defined in Eq. (2) have negative real parts $\text{Re}(\lambda) \leq 0$, and we sort them in absolute ascending order $|\text{Re}(\lambda_0)| \leq |\text{Re}(\lambda_1)| \leq \cdots$. The lowest eigenvalue $\lambda_0 = 0$ corresponds to ρ_{steady}, and the Liouvillian gap that determines the slowest decay rate to the steady state is given by $\lambda_{\text{ADR}} = \text{Re}(\lambda_1)$. The closing of the Liouvillian gap indicates a DPT [25]. In Fig. 1(e), λ_{ADR}

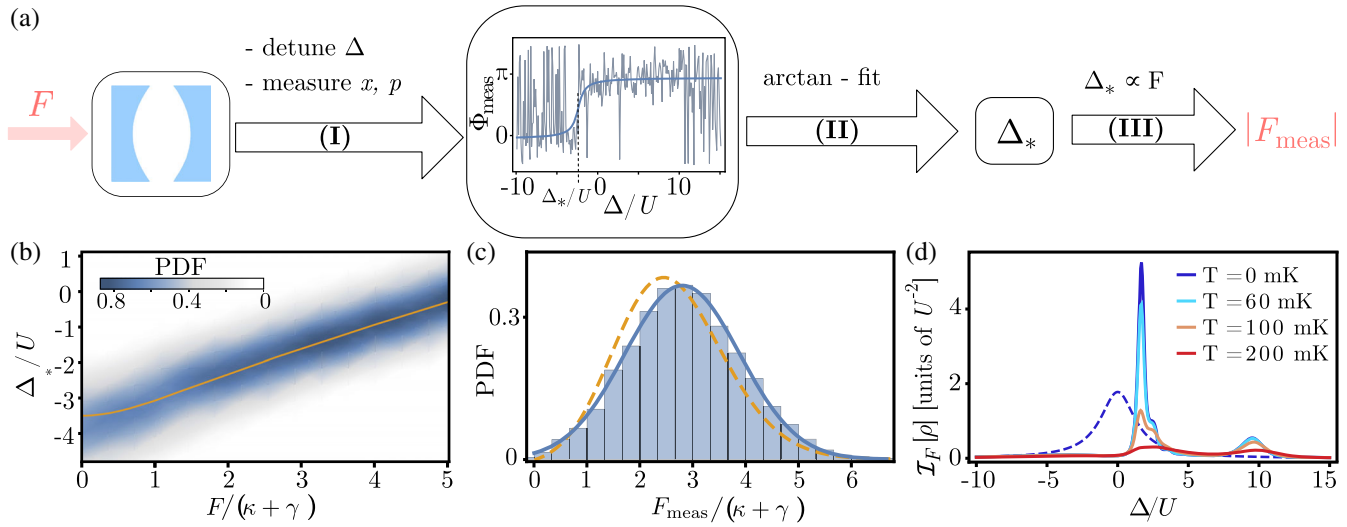

FIG. 2. (a) Measurement protocol: Φ is measured via heterodyne detection (gray) and Δ_* is extracted from an arctan fit (blue), which is then used to determine F_{meas} (for details, see the main text). (b) Δ_*/U as a function of F obtained from the master equation (2) (orange line) and its associated probability density function (PDF, blue) obtained from repeated heterodyne simulations (3). (c) PDF of F_{meas} for $F/U = 4$, i.e., $F/(\kappa+\gamma) = 2.67$; histogram from the simulated heterodyne detection (blue) and a fit to a Gaussian (blue line), with mean $\bar{F}_{\mathrm{meas}}/(\kappa+\gamma) = 2.79 \approx F/(\kappa+\gamma)$ and standard deviation $\Delta_{F_{\mathrm{meas}}}/(\kappa+\gamma) = 1.1$. The dashed line (orange) is the prediction based on the stochastic switching in the Husimi Q function; cf. Eq. (5). $\kappa/U = 1$ and the other parameters are the same as in Fig. 1. (d) Quantum Fisher information of estimating F in the steady state (6) as a function of Δ/U (solid lines) [32]. Note the prominent peak at $\Delta = \Delta_* \approx 0$ and a smaller one at $\Delta/U \approx 10$, corresponding to the crossovers Ⓐ and Ⓑ in Figs. 1(c) and 1(d). Both features vanish at sufficiently large temperatures T. For comparison, the results for $G = U = 0$ (harmonic oscillator) at $T = 0$ are plotted (dashed). The main peak is modulated by the resonances in the system [19,35]. Parameters are chosen as $F/U = 4.5$, $|G|/U = 3$, $\gamma/U = 3$, and $\eta = 0$.

is shown as a function of the phase θ of G and Δ/U. In the regime where the phase Φ switches abruptly, we find a vanishingly small Liouvillian gap $-10^{-6}\gamma$ consistent with the expected first-order transition [26–28]. Note that for $0 \lesssim \theta \lesssim \pi$ the Liouvillian gap does not close, indicating that the phase switching occurs only for $-\pi \lesssim \theta \lesssim 0$.

We now study if the phase switching persists beyond the steady state. This is particularly relevant for experiments, because the detuning is typically nonadiabatically varied in time. Simulating the full Lindblad time evolution (2) under a linear dynamical scan of Δ, we show that both $\langle n\rangle$ and Φ manifest a hysteresis cycle [Figs. 1(c) and 1(d)]. Such hysteretic behavior survives if the sweep duration is lower than $1/\lambda_{\mathrm{ADR}}$. The steady state is approached with increasing sweep duration [32]. On the upsweep, only the standard photon number drop at $\Delta \propto G/U$ occurs. Interestingly, for downsweeps, both a marked increase in $\langle n\rangle$ at $\Delta/U \approx 11$ and a kink in $\langle n\rangle$ concomitant with the phase switching are seen. This is the quantum analog of the double hysteresis recently discovered in the classical version of our model [26–28].

The frequency at which the phase switches by π for downsweeps is henceforth labeled by Δ_*. We find that, remarkably, $\Delta_* \propto F$ over a wide range of single-photon drive amplitudes and relative phases [Fig. 2(b)]. Departures from this linearity occur when F becomes comparable to γ and η. Consubstantial behavior is seen in the classical limit [26], but quantum fluctuations increase the linear range. The linear relation holds for a large range of sweep times, with minor dependences of $\partial\Delta_*/\partial F$ on the sweep time t_s [32]. The relation $F \propto \Delta_*$ originating from a phase-switching DPT is the key result of our work. This result can now be exploited to develop a quantum transducer for measuring forces.

Quantum transduction protocol.—To describe a realistic measurement of Φ, we simulate continuous observations of x and p as realized in heterodyne detection schemes [36]. The time evolution of ρ in the presence of the detector can be described by the stochastic master equation

$$d\rho = -i[H,\rho]dt + (\gamma+\kappa)\mathcal{D}[a]\rho dt + \eta\mathcal{D}[a^2]\rho dt + \sqrt{\frac{\kappa}{2}}(dW_x\mathcal{H}[a] + dW_p\mathcal{H}[-ia])\rho, \tag{3}$$

where $\mathcal{H}[a]\rho = a\rho + \rho a^\dagger - \mathrm{tr}[a\rho + \rho a^\dagger]$ and $W_{x,p}$ are Wiener processes with $\langle W_i(t)\rangle = 0$, $\langle W_i(t)^2\rangle = t$. The measurement process effectively increases the single-photon loss rate $\gamma \to \gamma + \kappa$, where κ is the emission rate to the heterodyne detector. The measured values are given by $x_{\mathrm{meas}} = x + \sqrt{2/\kappa}dW_x/dt$ and $p_{\mathrm{meas}} = p + \sqrt{2/\kappa}dW_p/dt$, leading to $\Phi_{\mathrm{meas}} = \arctan[p_{\mathrm{meas}}/x_{\mathrm{meas}}]$. A sample noisy phase measurement is shown in Fig. 2(a). Our sensing

protocol works as follows [Fig. 2(a)]: (I) $\Delta(t)$ is varied in a downsweep, and the phase Φ_{meas} is recorded; (II) to extract Δ_* from the noisy phase profile, we fit $\Phi_{\mathrm{meas}}(\Delta) = \arctan[A(\Delta - \Delta_*)] + C$ with fitting parameters Δ_*, A, and C; (III) the driving strength F_{meas} is then obtained using the quasilinear relation to Δ_* [Fig. 2(b)]. Repeating the protocol multiple times yields a probability density function (PDF) for Δ_*. It matches the result from the averaged master equation (2), demonstrating the robustness of our scheme against quantum noise from continuous measurements. Making use of the linear relation, the PDF for Δ_* can be translated into a PDF for F_{meas} [Fig. 2(c)]. The distribution can be approximated by a Gaussian with standard deviation $\Delta_{F_{\mathrm{meas}}} = 1.1(\kappa + \gamma)$ that marks the intrinsic quantum noise uncertainty that limits our measurement resolution. The simulations of the heterodyne detection were carried out with QuTiP [34].

We now show that the PDF obtained from the heterodyne detection can also be determined from the master equation (2) with $\gamma \to \gamma + \kappa$. First, the Husimi Q function can be interpreted as a probability density for continuous measurements [37–40]. As the Q function changes quadrant across the phase switch at $\Delta = \Delta_*$ [Fig. 1(b)], we introduce the following probabilities:

$$\mathcal{P}_{\Phi_-} = \int_{-\infty}^{+\infty} dp \int_{-\infty}^{0} dx Q(x, p) \tag{4}$$

and $\mathcal{P}_{\Phi_+} = 1 - \mathcal{P}_{\Phi_-}$, where $\mathcal{P}_{\Phi_{-(+)}}$ is the probability of measuring the phase in the left (right) half plane. Note that, when Δ is varied in time, the Husimi Q function and the corresponding $\mathcal{P}_{\Phi_\pm}$ are time dependent. Let $\mathcal{P}^i_m$ denote the probability to measure the phase $m = \Phi_\pm$ at time step i and $\mathcal{P}^{i \to i+1}_{m \to n}$ the probability to transition from phase $m = \Phi_\pm$ to phase $n = \Phi_\mp$ between time steps i and $i + 1$. Making the physically reasonable assumption that the system transitions preferably to the steady state, we obtain the following simple expression for the transition probability to switch from Φ_- to Φ_+ between the time steps i and $i + 1$ [32]:

$$\mathcal{P}^{i \to i+1}_{\mathrm{tr}} = \mathcal{P}^i_{\Phi_-} - \mathcal{P}^{i+1}_{\Phi_-}. \tag{5}$$

Consequently, for a linear sweep of the detuning, $\mathcal{P}_{\mathrm{tr}}(t) \propto \mathcal{P}_{\mathrm{tr}}[\Delta(t)] \equiv \mathcal{P}[\Delta_* = \Delta(t)]$. Making use of the linear relation $F \propto \Delta_*$ [Fig. 2(b)], we obtain the PDF of the measured F, $\mathcal{P}(F_{\mathrm{meas}}) \propto \mathcal{P}(\Delta_*)$. This simple result qualitatively agrees with the full PDF obtained from the heterodyne simulation [Fig. 2(c)]. When F is decreased to very low values, the contributions of both parametron modes to ρ become comparable and, consequently, strongly reduce the sensitivity of our protocol. Moreover, in this limit the approach based on Eq. (5) breaks down.

We note that F is the quantum optical equivalent of a classical mechanically oscillating force acting on a harmonic oscillator in the rotating-wave approximation [29]. The measurement protocol discussed here could thus be extended to mechanical forces as well. A candidate state-of-the-art system for force sensing is a laser-trapped nanoparticle, which can be parametrically driven [41]. We obtain the following parameters for our model: $\kappa = 2.5$ mHz, $\eta = 1.3$ mHz, $G = 15$ mHz, $U = 2.5$ mHz, mass $m = 3 \times 10^{-18}$ kg, and eigenfrequency $\omega_0 = 2.5 \times 10^5$ Hz. Simulating Eq. (3), we obtain the PDF for F_{meas}, which gives the sensitivity defined as $S = \Delta_F \sqrt{t_s} = 15\ \mathrm{yN}/\sqrt{\mathrm{Hz}}$. The sensitivity can be further improved by reducing η as well as increasing $|G|$. This is very competitive with state-of-the-art proposals for weak force measurements using quantum noise limited detectors [42]. Furthermore, a hallmark of our protocol is its robustness to the ubiquitous readout noise present in any measuring scheme [28]. This is attributable to the fact that the protocol depends on a π jump in the phase and not on any particular value of the phase. For completeness, we perform a quantitative analysis on the impact of readout noise and find that our sensing scheme is superior to standard linear force sensing schemes by a factor of ~ 2 in the signal-to-noise ratio [32]. This insensitivity to readout noise makes our method especially relevant for detecting weak drives.

Classical noise.—To substantiate the robustness of our proposal, we now investigate the influence of finite temperature on the phase switching in the KPO. Temperature can induce random switching between the parametron modes, thus potentially degrading the fidelity of the sensor. To quantify this, we include an additional dissipative process in the master equation such that $\dot{\rho} = -i[H, \rho] + \gamma(1 + n_{\mathrm{th}}) \mathcal{D}[a]\rho + \gamma n_{\mathrm{th}} \mathcal{D}[a^\dagger]\rho$ with $n_{\mathrm{th}} = n_{\mathrm{th}}(\beta\omega_c)$ the thermal number of photons at the real frequency of the KPO ω_c, $\beta = k_B T$, and T the temperature of the environment. For simplicity, we assume $\eta = 0$, since the dominant noise channel is typically single-photon loss [20]. A useful measure to quantify the sensitivity of our protocol for various temperatures is the quantum Fisher information (QFI). It is used to analyze phase transitions [4,5,43–45] and provides a measure of the variance of parameter estimations in quantum sensing and metrology [46,47]. Since our sensing scheme relies on a phase transition, the QFI of the steady state ρ is particularly appropriate for investigating the role of temperature on the quantum transducer. The QFI quantifies the change of the steady-state density matrix $\rho = \sum_i \lambda_i |\psi_i\rangle \langle\psi_i|$ with respect to variations in the parameter to be estimated and, in our case, takes the form defined as

$$\mathcal{I}_F[\rho] = 2 \sum_{ij, \lambda_i + \lambda_j \neq 0} \frac{|\langle\psi_i|\partial\rho/\partial F|\psi_j\rangle|^2}{\lambda_i + \lambda_j}, \tag{6}$$

for the estimation of F.

In Fig. 2(d), we present our results for the temperature-dependent QFI for another state-of-the-art KPO realized in

circuit QED. Using circuit-QED parameters $\omega_c = 7.5 \times 2\pi$ GHz and $U = 25$ kHz [20], we see that the QFI at $T = 0$ (blue) exhibits two sharp peaks in correspondence with the crossovers discussed in Fig. 1. Note that the QFI is largest around $\Delta = \Delta_* \sim 0$, where the phase switches, while the usual bistability transition where the photon number jumps at larger Δ exhibits a lower QFI. This shows the high information content in the vicinity of the DPT. The QFI of our sensing scheme is, therefore, substantially higher than that of the standard linear force sensing with the linear oscillator (dashed blue). The QFI progressively decreases with the temperature, indicating an increasing lower bound for the force estimation variance Δ_F. This bound, however, remains remarkably low for the typical operating temperature of circuit-QED devices, $T \approx 20$ mK. This illustrates the potency of our sensing protocol based on a DPT for sensitive measurements.

Outlook.—We have proposed a quantum sensing scheme that relies on the heightened sensitivity of driven DPTs. Our transduction scheme is widely realizable in contemporary quantum engineered devices, including optical [6,7], mechanical [41,48], and electronic [10,20] platforms. A key ingredient for our proposal relies on the control of single- and two-photon drives, which are readily accessible in such systems using standard nonlinear wave-mixing techniques [49]. Optimizing the Kerr nonlinearity and the two-photon drive can further improve the protocol. Our work opens interesting perspectives in studying the interplay of sensing and entanglement in networks of KPOs *vis-à-vis* synchronization and other collective many-body effects [50–53].

We thank L. Papariello and A. Eichler for fruitful discussions. We acknowledge financial support from the Swiss National Science Foundation through Grant No. PP00P2_163818 and No. CRSII5_177198.

[1] C. L. Degen, F. Reinhard, and P. Cappellaro, Rev. Mod. Phys. **89**, 035002 (2017).
[2] P. Zanardi, M. G. A. Paris, and L. Campos Venuti, Phys. Rev. A **78**, 042105 (2008).
[3] Z.-P. Liu, J. Zhang, Ş. K. Özdemir, B. Peng, H. Jing, X.-Y. Lü, C.-W. Li, L. Yang, F. Nori, and Y.-x. Liu, Phys. Rev. Lett. **117**, 110802 (2016).
[4] K. Macieszczak, M. Guţă, I. Lesanovsky, and J. P. Garrahan, Phys. Rev. A **93**, 022103 (2016).
[5] S. Fernández-Lorenzo and D. Porras, Phys. Rev. A **96**, 013817 (2017).
[6] M. J. Hartmann, J. Opt. **18**, 104005 (2016).
[7] C. Noh and D. G. Angelakis, Rep. Prog. Phys. **80**, 016401 (2017).
[8] H. Ritsch, P. Domokos, F. Brennecke, and T. Esslinger, Rev. Mod. Phys. **85**, 553 (2013).
[9] R. Blatt and C. F. Roos, Nat. Phys. **8**, 277 (2012).
[10] S. Schmidt and J. Koch, Ann. Phys. (Amsterdam) **525**, 395 (2013).
[11] I. Carusotto and C. Ciuti, Rev. Mod. Phys. **85**, 299 (2013).
[12] H. M. Gibbs, S. L. McCall, and T. N. C. Venkatesan, Phys. Rev. Lett. **36**, 1135 (1976).
[13] P. D. Drummond and D. F. Walls, J. Phys. A **13**, 725 (1980).
[14] G. Rempe, R. J. Thompson, R. J. Brecha, W. D. Lee, and H. J. Kimble, Phys. Rev. Lett. **67**, 1727 (1991).
[15] W. Casteels, F. Storme, A. Le Boité, and C. Ciuti, Phys. Rev. A **93**, 033824 (2016).
[16] W. Casteels, R. Fazio, and C. Ciuti, Phys. Rev. A **95**, 012128 (2017).
[17] F. Minganti, N. Bartolo, J. Lolli, W. Casteels, and C. Ciuti, Sci. Rep. **6**, 26987 (2016).
[18] M. Elliott and E. Ginossar, Phys. Rev. A **94**, 043840 (2016).
[19] N. Bartolo, F. Minganti, W. Casteels, and C. Ciuti, Phys. Rev. A **94**, 033841 (2016).
[20] Z. Leghtas, S. Touzard, I. M. Pop, A. Kou, B. Vlastakis, A. Petrenko, K. M. Sliwa, A. Narla, S. Shankar, M. J. Hatridge, M. Reagor, L. Frunzio, R. J. Schoelkopf, M. Mirrahimi, and M. H. Devoret, Science **347**, 853 (2015).
[21] H. Goto, Phys. Rev. A **93**, 050301(R) (2016).
[22] S. Puri, S. Boutin, and A. Blais, npj Quantum Inf. **3**, 18 (2017).
[23] T. Inagaki, K. Inaba, R. Hamerly, K. Inoue, Y. Yamamoto, and H. Takesue, Nat. Photonics **10**, 415 (2016).
[24] S. E. Nigg, N. Lörch, and R. P. Tiwari, Sci. Adv. **3**, e1602273 (2017).
[25] E. M. Kessler, G. Giedke, A. Imamoglu, S. F. Yelin, M. D. Lukin, and J. I. Cirac, Phys. Rev. A **86**, 012116 (2012).
[26] L. Papariello, O. Zilberberg, A. Eichler, and R. Chitra, Phys. Rev. E **94**, 022201 (2016).
[27] A. Leuch, L. Papariello, O. Zilberberg, C. L. Degen, R. Chitra, and A. Eichler, Phys. Rev. Lett. **117**, 214101 (2016).
[28] A. Eichler, T. L. Heugel, A. Leuch, C. L. Degen, R. Chitra, and O. Zilberberg, Appl. Phys. Lett. **112**, 233105 (2018).
[29] P. A. Ivanov, N. V. Vitanov, and K. Singer, Sci. Rep. **6**, 28078 (2016).
[30] C. Macklin, K. O'Brien, D. Hover, M. E. Schwartz, V. Bolkhovsky, X. Zhang, W. D. Oliver, and I. Siddiqi, Science **350**, 307 (2015).
[31] F. Minganti, A. Biella, N. Bartolo, and C. Ciuti, Phys. Rev. A **98**, 042118 (2018).
[32] See Supplemental Material at http://link.aps.org/supplemental/10.1103/PhysRevLett.123.173601 for additional details on the numeric calculations, the sweep time, the dissipation coefficients, the derivation of the transition probability, the calculations of the QFI, and the readout noise, which includes Refs. [33,34].
[33] G. Salvatori, A. Mandarino, and M. G. A. Paris, Phys. Rev. A **90**, 022111 (2014).
[34] J. Johansson, P. Nation, and F. Nori, Comput. Phys. Commun. **184**, 1234 (2013).
[35] M. Biondi, G. Blatter, H. E. Türeci, and S. Schmidt, Phys. Rev. A **96**, 043809 (2017).
[36] H. M. Wiseman and G. J. Milburn, *Quantum Measurement and Control* (Cambridge University Press, Cambridge, England, 2009).
[37] U. Leonhardt and H. Paul, Prog. Quantum Electron. **19**, 89 (1995).
[38] J. Shapiro and S. Wagner, IEEE J. Quantum Electron. **20**, 803 (1984).

[39] S. Stenholm, Ann. Phys. (N.Y.) **218**, 233 (1992).
[40] S. L. Braunstein, C. M. Caves, and G. J. Milburn, Phys. Rev. A **43**, 1153 (1991).
[41] J. Gieseler, M. Spasenović, L. Novotny, and R. Quidant, Phys. Rev. Lett. **112**, 103603 (2014).
[42] P. A. Ivanov, Phys. Rev. A **94**, 022330 (2016).
[43] T.-L. Wang, L.-N. Wu, W. Yang, G.-R. Jin, N. Lambert, and F. Nori, New J. Phys. **16**, 063039 (2014).
[44] U. Marzolino and T. Prosen, Phys. Rev. B **96**, 104402 (2017).
[45] I. Frérot and T. Roscilde, Phys. Rev. Lett. **121**, 020402 (2018).
[46] C. W. Helstrom, *Quantum Detection and Estimation Theory* (Academic, New York, 1976).
[47] S. L. Braunstein and C. M. Caves, Phys. Rev. Lett. **72**, 3439 (1994).
[48] M. Rossi, D. Mason, J. Chen, Y. Tsaturyan, and A. Schliesser, Nature (London) **563**, 53 (2018).
[49] Y. Shen, *The Principles of Nonlinear Optics* (Wiley, New York, 1984).
[50] T. E. Lee, C.-K. Chan, and S. Wang, Phys. Rev. E **89**, 022913 (2014).
[51] V. Savona, Phys. Rev. A **96**, 033826 (2017).
[52] M. Biondi, E. P. L. van Nieuwenburg, G. Blatter, S. D. Huber, and S. Schmidt, Phys. Rev. Lett. **115**, 143601 (2015).
[53] F. Baboux, L. Ge, T. Jacqmin, M. Biondi, E. Galopin, A. Lemaître, L. Le Gratiet, I. Sagnes, S. Schmidt, H. E. Türeci, A. Amo, and J. Bloch, Phys. Rev. Lett. **116**, 066402 (2016).